Leber hereditary optic neuropathy mutations in the ND6 subunit of mitochondrial complex I affect ubiquinone reduction kinetics in a bacterial model of the enzyme

Jukka Pätsi, Marko Kervinen, Moshe Finel, Ilmo E. Hassinen

Biochemical Journal Immediate Publication. Published on 26 Sep 2007 as manuscript BJ20070866

Leber hereditary optic neuropathy mutations in the ND6 subunit of mitochondrial complex I affect ubiquinone reduction kinetics in a bacterial model of the enzyme

Jukka PÄTSI[1], Marko KERVINEN[1,2], Moshe FINEL[3] and Ilmo E. HASSINEN[1,4]

[1]Department of Medical Biochemistry and Molecular Biology, University of Oulu, P.O. Box 5000, FIN-90014 Oulu, Finland, [2]Oulu Eye Research Unit, Department of Ophthalmology, University of Oulu, FIN-90014 Oulu, Finland, and
[3]Drug Discovery and Development Technology Center, Faculty of Pharmacy, University of Helsinki, P.O. Box 56, FIN-00014 Helsinki, Finland.

[4]To whom correspondence should be addressed:
Ilmo E. Hassinen, M.D., Ph.D.
Department of Medical Biochemistry and Molecular Biology
University of Oulu
P.O. Box 5000
Street address: Aapistie 7
FIN-90014 Oulu, Finland
tel. +358-8-5375802
fax +358-8-5375811
E-mail: ilmo.hassinen@oulu.fi

SYNOPSIS

Leber hereditary optic neuropathy (LHON) is a maternally inherited disease that leads to sudden loss of central vision at a young age. There are three common primary LHON mutations, occurring at positions 3460, 11778 and 14484 in the human mitochondrial DNA, leading to amino acid substitutions in mitochondrial complex I subunits ND1, ND4 and ND6, respectively. We have now examined the effects of ND6 mutations on the function of complex I using the homologous NuoJ subunit of *Escherichia coli* NDH-1 as a model system. The assembly level of the NDH-1 mutants was assessed using electron transfer from deamino-NADH to the "shortcut" electron acceptor hexammine ruthenium, whereas ubiquinone reductase activity was determined using decylubiquinone as a substrate. Mutant growth in minimal medium with malate as the main carbon source was used for initial screening of the efficiency of energy conservation by NDH-1. The results indicated that NuoJ-M64V, the equivalent of the common LHON mutation in ND6, had a mild effect on *E. coli* NDH-1 activity, while nearby mutations, particularly NuoJ-Y59F, NuoJ-V65G and NuoJ-M72V, severely impaired the decylubiquinone reduction rate and cell growth on malate. NuoJ-M64 and NuoJ-M72 position mutants lowered the affinity of NDH-1 for decylubiquinone and explicit C- type inhibitors, whereas NuoJ-Y59C displayed substrate inhibition by oxidized decylubiquinone. The results are compatible with the notion that the ND6 subunit delineates the binding cavity of ubiquinone substrate, but does not directly take part in the catalytic reaction. How these changes in the enzyme's catalytic properties contribute to LHON pathogenesis is discussed.

PAGE HEADING: LHON mutation modelling in *Escherichia coli*

KEY WORDS: NADH:ubiquinone oxidoreductase, mitochondrial DNA, mitochondrial disease, Escherichia coli, Leber hereditary optic neuropathy, enzyme inhibitors.

#Abbreviations

d-NADH, deamino-NADH (nicotinamide-hypoxanthine dinucleotide (reduced form)); DB, decylubiquinone (2,3-dimethoxy-5-methyl-6-decyl-1,4-benzoquinone); HAR, hexammine ruthenium; LHON, Leber hereditary optic neuropathy; LDYT, Leber hereditary optic neuropathy and/or dystonia; MELAS, Mitochondrial encephalomyopathy, lactic acidosis and stroke like episodes; MES, morpholinoethanesulfonic acid; mtDNA, mitochondrial DNA; PMSF, phenylmethylsulfonylfluoride; Q_1, ubiquinone-1; Q_{10}, ubiquinone-10; VNA, *n*-vanillylnonanamide.

INTRODUCTION

Leber hereditary optic neuropathy (LHON) is a maternally inherited human disease causing acute to subacute bilateral painless loss of central vision in young adults, with male predominance. After the acute phase, optic nerve atrophy and centro-cecal absolute scotoma develop within weeks in one eye, followed by the other eye after a mean interval of two months [1]. The final visual outcome varies, and patients occasionally experience a marked visual recovery after the acute phase, both being dependent on the genotype [2]. The underlying genetic cause in LHON is a mutation in the mitochondrial genome. The first reported mutation linked to LHON was G11778A [3], and this and two other missense mutations, G3460A and T14484C, currently account for 96% of all patients diagnosed [4], so that they are classified as common primary mutations.

Mitochondrial NADH:ubiquinone oxidoreductase (complex I, E.C. 1.6.5.3) extracts electrons from NADH and channels them through FMN and a set of serially arranged iron-sulfur clusters to the reduction site of the lipophilic electron acceptor ubiquinone [5]. The energy liberated in this electron transfer is used to drive proton pumping across the mitochondrial inner membrane with a stoichiometry of $4H^+/2e^-$ [6]. It is a multi-subunit enzyme with 45 dissimilar proteins [7], fourteen of which comprise the evolutionally conserved catalytic core, which is also found in NDH-1, the bacterial counterpart of the mitochondrial complex I, see [8] for a review. In mitochondrial complex I seven of these 14 core subunits are encoded by the mitochondrial genome and synthesized within the organelle [9]. All these seven subunits, designated ND1-ND6 and ND4L, are integral membrane proteins having 3 to 14 transmembrane segments [10].

The common primary LHON mutations occur in three subunits of complex I, namely ND1, ND4 and ND6, all of which belong to the membrane domain of the enzyme. Several additional LHON-associated replacement mutations have been found in other mitochondrially encoded subunits of complexes I, III, IV and F_1F_o-ATP-synthase [11]. Taking all the known LHON mutations into account, it appears that the ND1 and ND6 genes are the main "hot spots" for such mutations [12,13], since a total of 16 of their codons have been identified as being associated with LHON (Mitomap, www.mitomap.org May 2007). Interestingly, many of the pathogenic ND6 subunit mutations are located in the relatively highly conserved N-terminal region within its third transmembrane helix (Figure 1).

(Place Figure 1 here.)

Several hypotheses have been proposed regarding the primary cause of the disease phenotype. These include mild impairment of mitochondrial respiration due to a complex I defect, as found in the

ND1-A52T and ND4-R340H mutations [14] but not in ND6-M64V [15,16]. A defect in ATP production with unaltered ATP content has been found in trans-mitochondrial hybrid cell lines carrying any of the common LHON mutations [17,18]. Increased production of reactive oxygen species (ROS) or increased sensitivity to oxidative stress has been found in a ND1-A52T and ND4-R340H mutant cybrid neuronal cell model [19], whereas ROS production was not markedly increased in a ND6-M64V mutant cell line [20]. Cell death in LHON appears to occur by an apoptotic mechanism [21,22], but it remains obscure how the apoptotic wave of cell death is initiated exclusively in the retinal ganglion cells, especially in the case of the mild ND6-M64V mutation.

The mitochondrial genome accumulates mutations at a rate approximately an order of magnitude faster than the nuclear genome, and it is difficult to distinguish between rare haplogroup-specific variants and true pathogenic LHON mutations [23]. The pathogenic mutations are also frequently accompanied by other genetic alterations in mtDNA and the contribution of individual mutations to the clinical phenotype and the biochemical defect may be difficult to establish. It is also very difficult to introduce site-specific mutations into the mitochondrial genome, so that we employed a bacterial homologue of complex I, the NDH-1 of *Escherichia coli*, as a model system for studying the effects of LHON and other mutations in the NuoJ subunit, the bacterial counterpart of ND6, on the function of the enzyme. The method allows us to examine the putatively pathogenic mutations against a truly neutral background and to explore their effects on the enzyme catalytic turnover in detail.

A bacterial system has been employed on several occasions to model disease mutations. During the execution of the present study, which started during our endeavours with site-directed mutagenesis of the NuoK subunit [24], Kao and coworkers [25] reported on the modeling of mutations in the NuoJ subunit in *E. coli*, and our study, carried out using the methodology we had developed for NuoK [24], may also be partly regarded as an extension of the experiments of Kao and coworkers on NuoJ [25]. We have now analyzed the *E. coli* equivalent of the common LHON mutation 14484/ND6-M64V as well as several other point mutations its vicinity. This is important, because a knowledge of the pathophysiology of LHON is currently insufficient and the delineation between pathogenic mutations and polymorphism is difficult, so that the purported role of some mtDNA mutations in the development of LHON has recently been challenged [26].

EXPERIMENTAL

Materials

Decylubiquinone (DB)[#], NADH, deamino-NADH (d-NADH), DL-malate, piericidin A, soybean phospholipids (Asolectin), *N*-vanillylnonanamide (VNA), stigmatellin and myxothiazol were from Sigma. HAR was purchased from Aldrich, HEPES and MES from AppliChem, and potassium cyanide

and PMSF from Merck. Oligonucleotides were purchased from Sigma-Genosys, the QuikChange XL mutagenesis kit was from Stratagene and the annonin extract was a generous gift from Dr. Y. K. Gupta, Varanasi, India.

Mutagenesis

A series of site-directed mutants was generated employing the same strategy as was applied earlier to the study of mutations in the NuoK subunit of *E. coli* NDH-1, an equivalent of the ND4L subunit of complex I [24]. The point mutations listed in Table 1 were introduced into pJK [24] using the QuikChange XL mutagenesis kit (Stratagene) according to the manufacturer's instructions, followed by DNA sequencing of the construct. The oligonucleotides used in mutagenesis are listed in supplementary Table S1. Wild-type or mutant *nuoJ* in conjunction with non-mutant *nuoK* (with the c-terminal His-tag) were transformed into GvnuoJK [24], a *nuoJK* knockout strain, for *in trans* complementation. It should be noted that the parent strain used here carries only the *bd* type of ubiquinol oxidase in the aerobic respiratory chain [27].

(Place Table 1 here.)

Bacterial culture and membrane preparation

For membrane preparation, a colony from a fresh transformation plate was grown overnight in LB medium in the presence of streptomycin, ampicillin and 1% arabinose and diluted 1:100 in fresh LB medium supplemented with streptomycin and ampicillin. After 6 to 8 hours of cultivation, a fraction of this LB culture was diluted 1:100 in malate-YE medium (65 mM potassium phosphate buffer supplemented with 90 mM DL-malate as the main carbon source, 0.1% (w/v) yeast extract, 1 mM citrate, 75 mM ammonium sulphate, salts and ampicillin) [24], and grown at 37°C under high aeration. The cells were collected (4200×g, 20 min, 4°C) when the attenuance at 600 nm (D_{600}) reached 0.1-0.4, cooled, and washed with 50 mM MES/KOH, pH 6.5, 2.5 mM EDTA and 0.2 mM PMSF. The washed cells were used for membrane preparation according to [28], except that 50 mM MES/KOH, pH 6.5, 0.2 mM PMSF, 5 mM $MgSO_4$ and 10 µg/ml DNAse I were used during the French Press treatment. Unbroken cells and debris were removed by centrifugation (4 200×g, 20 min), only the supernatant was used for ultracentrifugation (180 000×g, 65 min) and the membranes were suspended in 50 mM MES/KOH, pH 6.5, containing PMSF as above, to about 0.5 ml per gram of initial cell weight. Membrane samples for the inhibitor titration experiments were prepared as described in [29]. The protein concentration in the membrane preparations was assessed according to Lowry [30]. Growth on malate was determined as the final attenuance of the culture at 600 nm (D_{600}) after 24 h of growth in malate-YE medium at 37°C.

Activity measurements

E. coli possesses two NADH:quinone oxidoreductases, NDH-1 and NDH-2. The former is an equivalent of complex I, while the latter is a single-subunit enzyme that, although catalyzing electron transfer from NADH to ubiquinone, does not couple the electron transfer activity to proton translocation across the membrane or to the generation of a membrane potential [31]. The two *E. coli* NADH oxidases can be distinguished from each other in activity assays by employing the non-physiological NADH analogue deamino-NADH (d-NADH) as a substrate, since this serves as an equally good electron donor for NDH-1 as NADH, whereas NDH-2 is unable to oxidize it. Accordingly, d-NADH was used as a substrate to measure NDH-1-dependent activities, while NADH was employed to assay the combined NDH-1 and NDH-2 capacity, which corresponds better to the in vivo situation during bacterial growth.

The activity assays were performed on a dual-wavelength spectrophotometer as previously described [24], with the modifications that the d-NADH:DB oxidoreductase assays were performed with freshly prepared membrane samples in the presence of 0.1 mg/ml membrane protein, 0.5 mg/ml soybean phospholipid and 90 μM deamino-NADH. Six DB concentrations, ranging from 50 to 600 μM, were used and three parallel experiments were performed at each concentration. The rates of DB reduction in the concentration range between 0.5 to 45 μM were estimated from the progress curve throughout the course of a complete reaction (in triplicate), the initial DB concentration being 30 to 45 μM. Three to five colonies for each mutant or control were analyzed independently. The VNA sensitivity at 100 μM DB was tested by adding VNA to a final concentration of 400 μM after recording the initial DB-reductase activity for one to two minutes. For the d-NADH:HAR activity, the previously used annonin was replaced by 400 μM VNA. In the sensitivity tests the inhibitors dissolved in ethanol or DMSO to a final concentration of 30-400 μM VNA, 0.5-20 μg/ml annonin, 0.5-19 μM piericidin A, 5-100 μM stigmatellin or 5-100 μM myxothiazol (or an equal amount of ethanol or DMSO) were added before DB and the assays were conducted similarly to the d-NADH:DB oxidoreductase assays in all other aspects. The DB concentration was determined spectrophotometrically using an extinction coefficient of 14.0 mM^{-1} cm^{-1} at 278 nm.

Statistics

Student's t-test for independent samples was used to compare two groups. For multiple comparisons, one-way ANOVA followed by the Dunnett test was used. Curves were fitted to the kinetic equation with Sigmaplot 9.0 (Systat Software, Erkrath, Germany).

RESULTS

Growth and NADH oxidation capacity

On the basis of our previous experiments on NuoK mutagenesis in *E. coli*, the inability to grow on malate is a useful measure of the energy conserving function of NDH-1 [24]. Therefore the effects of mutations on complex I activity were first evaluated by testing their effect on cell growth in a minimal medium where malate was the main carbon source. The results, depicted in Figure 2, show that there is a positive sigmoidal correlation between d-NADH oxidase activity and cell growth measured as attenuance at 600 nm ($r= 0.796$, $P<0.001$). Interestingly, the growth of the double mutant M64V/M72A on malate as the main carbon source, and also the d-NADH:O_2 activity, were lower than for either mutant alone (Table 2).

(Place Figure 2 here.)

(Place Table 2 here.)

Among the set of NuoJ mutants produced, Y59F and V65G exhibited a knock-out-like growth pattern, while the final D_{600} of the M72V mutant in the malate-YE medium was only slightly higher (Table 2). To test whether the poor growth capacity of these mutants was due to a deficiency in the respiratory chain downstream from the NDH-1 site or to NDH-1 itself, their NADH:O_2 activities were measured (Table 2). Subtraction of the d-NADH:O_2 activity from the NADH:O_2 activity gives an estimate of the NDH-2linked respiration by-passing the NDH-1 coupling-site, and this turned out to be even higher in the Y59F, V65G and M72V mutants than in the controls (results not shown), demonstrating that apart from NDH-1, the respiratory complexes were functioning normally in these mutants.

Expression and assembly

The hexammine ruthenium reductase activity (d-NADH:HAR) in the membranes (Table 2) was used to estimate the level of expressed and assembled NDH-1, since its loss through *nuoJK* knock-out could be restored by complementation *in trans* [24]. Despite the impaired malate growth, mutants Y59F and M72V exhibited considerable d-NADH:HAR reductase activity, similar to the control or mutants such as Y59C that grew much better on malate. Even in the case of V65G, the poorest-growing mutant, the d-NADH:HAR reductase activity was higher than in the double mutant M64V/M72A, although the latter, but not the former, grew reasonably well on malate (Table 2).

The results also revealed great variability in expression and assembly levels between membrane batches of individual mutants. Due to this observation, the d-NADH:DB activity of each batch of membranes was normalized to the corresponding HAR reduction activity (by taking the activity ratio) in order to better reveal changes in enzyme catalysis.

Ubiquinone reduction and binding

The d-NADH:DB reductase activity and its dependence on the electron acceptor concentration were measured in isolated membranes from the various strains (Table 3). Complementation of the knock-out with wild type *nuoJK* construct (control in Table 3) resulted in 34% of the assembly normalized NDH-1 activity in the parent strain GV102 under same conditions [29]. Reason for this is currently unsolved, but it may partly be due to non-synchronised expression and assembly of NDH-1 subunits from *nuo*-operon and the plasmid. Assembly normalized NDH-1 activities were, however, constant in control complementations with *nuoJK* expression plasmid introducing a C-terminal His_6-tag into NuoK present in all NDH-1 enzymes analyzed in this study or with a plasmid where the original stop-codon was reintroduced into *nuoK* (Kervinen, unpublished results). Therefore, we consider it justified to use this system to evaluate the effects of site-directed mutations on NDH-1, and the results obtained with different mutants were compared to the wild-type complementation throughout this study.

(Place Table 3 here.)

As compared with the method used by us previously [24], the changes to the membrane preparation procedure (omission of EDTA, addition of Mg^{2+} and avoidance of freezing of the sample before the assay) resulted in higher respiratory chain activities and made it possible to perform more detailed analyses of NDH-1 function. The results demonstrated that one mutant, V65G, was practically devoid of d-NADH:DB reductase activity (5.5 ± 0.6 nmol min^{-1} mg^{-1} at 100 μM DB *versus* 196 ± 22 nmol min^{-1} mg^{-1} in the control), and that this was not stimulated by higher DB concentrations (results not shown). No accurate analysis of the DB reduction kinetics could be performed in this case, however. Mutant Y59F exhibited the lowest (corrected) V_{max} value, while the V_{max}/HAR ratio was also significantly reduced in mutants M64C, M72V, and M72C (Table 3). The same pattern was observed in the assembly-corrected d-NADH oxidase activities in these mutants (with endogenous ubiquinone as a substrate), the ratios of d-NADH:O_2 activity to the HAR reduction rate being 47%, 38% and 51% of the control, respectively. Unlike the other mutants and the control, Y59C and Y59F showed higher NDH-1 activities with the endogenous electron acceptor than with DB as compared with the wild-type control (93% of wild type activity with endogenous ubiquinone *versus* 73% (V_{max}/HAR) with DB, and 45% with endogenous ubiquinone *versus* 38% with DB, in Y59C and Y59F, respectively).

An interesting finding was that some mutations led to a clear substrate inhibition by oxidized decylubiquinone (Figure 3). This was analyzed by fitting the data to the equation

$$v = V_{max}\cdot[S]/(K_m+[S]+([S]^2/K_s'))\quad \text{(Eq. 1)},$$

where K_s' is the equilibrium constant for binding of a second substrate molecule to the active site of the enzyme-substrate complex [32]. The results are listed in Table 3. The K_m value for the wild type control was in the range 16 to 25 μM. All the M64, M72, and Y109-position mutants and also the double mutant M64V/M72A exhibited a higher K_m value for this ubiquinone analogue (Table 3), suggesting somewhat lower affinity for the physiological electron acceptor as well. Mutations at Y59 did not have a significant effect on the K_m value, but, in contrast, showed the largest increase in sensitivity to substrate inhibition by DB, the Y59C mutant having the clearest effect (Table 3 and Figure 3). The double mutant M64V/M72A also showed some increase in sensitivity to substrate inhibition, higher than with either of the mutations alone, but the difference in K_s' was not statistically significant as compared with the control. Additionally, all position M72 substitutions which led to an increased K_m for DB also showed a tendency for an increase in K_s'.

(Place Figure 3 here.)

The d-NADH:HAR, d-NADH:O_2, NADH:O_2 and d-NADH:DB activities in the control and the mutants growing poorly on malate, namely Y59F, V65G and M72V, were also analyzed in membranes from cells grown on LB medium and were very similar to the results for the respective membrane batches prepared from cells grown in the malate-YE medium, as listed in Tables 2 and 3.

Inhibitor sensitivity

The sensitivity of the d-NADH:DB oxidoreductase activity to 400 μM VNA in the mutants did not differ much from the wild type (percentage inhibition of the initial rate was 73-84%), except perhaps in Y59F (66-74%). Titration experiments in the presence of 100 μM DB and 90 μM d-NADH showed, however, that the I_{50} (the inhibitor concentration that produces 50% inhibition of the activity) for VNA in mutant Y59F was very similar to the control value, 56 μM and 62 μM, respectively. We selected M72V, the counterpart of the disease-associated ND6-A72V mutant, for further inhibitor sensitivity experiments because this mutant showed the largest decrease in DB affinity. Sensitivity was tested for class I/A-type and C-type inhibitors and for stigmatellin and myxothiazol, which interact at or near the ubiquinone-binding site(s). The results indicate a clear increase in the I_{50} value of mutant M72V for both annonin and VNA, but not for piericidin A, stigmatellin or myxothiazol (Table 4). It should be noted here that an equal amount of membrane protein was used in the cuvette

for each of the mutants or control and excess phospholipid was added in both the DB binding and inhibitor sensitivity experiments in order to eliminate the effect of changes in lipid content between separate samples.

(Place Table 4 here.)

DISCUSSION

Despite an abundance of research into the pathophysiology of LHON, the underlying cause of the onset of neuronal cell death remains obscure and the biochemical defects at the level of complex I are controversial. We have developed a disease model in *E. coli* in which we can estimate and compare the effects of different LHON mutations (including the rare ones) on complex I activity against a genetically neutral background without the contribution of other mitochondrial or nuclear DNA mutations. A similar approach was used recently to investigate the effects of amino acid changes within the ND1 subunit causing MELAS syndrome [29]. The effect of mutated mtDNA against neutral nuclear background can be studied even in mammalian cells using cybrid techniques and haplotype-matched controls, although lack of the possibility of its site-directed mutagenesis remains a shortcoming. A few mtDNA mutations have been found in derivatives of murine cell lines after culturing under conditions selective for defects in cell respiration, and random mutagenesis can be used in combination of production of transmitochondrial cybrids [33,34]. Human colonocytes from aged individuals harbour mtDNA mutations and can be studied experimentally in cybrid cells, but they are different from those occurring in proven inherited mitochondrial disease [35]. Therefore, focusing on a spectrum of defined mtDNA mutations is difficult on a neutral genetic background when one uses in vitro eukaryotic models. Although restricted to the structural genes of the respiratory enzymes and mainly to the effects expressed at the enzymatic level, use of bacterial models makes it possible to study also more deleterious substitutions than those caused by the naturally occurring mtDNA mutations and may therefore be a more useful model in elucidating the catalytic function of complex I.

In trans complementation of the *nuoJK* knockout strain was used here to introduce several replacement mutations into NuoJ, the *E.coli* counterpart of human ND6, at sites corresponding to the LHON mutations, residues Y59, M64 and A72, and in some nearby residues, in order to investigate the effects of these amino acid substitutions on NDH-1 activity. It may be noted here that Kao and coworkers [25] have recently inserted mutations directly into the *nuoJ* gene of the *E. coli* genome. Importantly, the DB reductase activities in the Y59C, Y59F, M64V and V65G generated by Kao et al. [25] and in this study by means of in-trans complementation were comparable, so that it may be

concluded that these two methods are equally applicable. In order to understand the nature of the effect these mutations have on the enzyme, we performed a further analysis of the mutants compared with the previous work of Kao et al. [25] by determining the NDH-1-dependent growth phenotype and kinetic parameters for the mutant enzymes in question, and probed the selected mutant enzymes with a series of NDH-1 specific inhibitors.

Substitution of glycine for V65 had deleterious effects on NDH-1, in agreement with previous findings (see above), and the NDH-1 activity in this mutant was not ameliorated by higher DB concentrations, which suggests that the defect brought about by the substitution is not probably due to a change in DB affinity, although no detailed analysis of DB binding could be performed. Many of the other mutations generated in the present work affected DB binding by NDH-1. The ubiquinone binding cavity in complex I is assumed to be large and elongated, harboring three overlapping inhibitor-binding sites [36,37]. It has been concluded on the basis of changes in inhibitor affinities in several mutants that the ubiquinone-binding site resides in the contact region between the 49kD and PSST subunits in the hydrophilic part, or at the interface between the hydrophilic part and the membrane arm, see Brandt 2006 for a review [38]. Although the location of the ND6 subunit with respect to the hydrophilic part is currently unknown, some evidence for it contributing to ubiquinone binding has been presented. In cybrid submitochondrial particles carrying an A72V mutation in ND6, substrate and product inhibition by decylubiquinone and decylubiquinol, respectively, have been observed [39]. Contrary to this, substitutions at M72 of *E.coli* NuoJ in the present study did not cause any substrate inhibition by DB, but instead induced a 1.7-2.0-fold increase in K_m for DB and lowered the affinity for binding a second substrate molecule at the active site, as well as affecting inhibitor resistance (Tables 3 and 4). There are no clinical studies on ubiquinone binding in the 14484/ND6-M64V mutant, although a change in this was proposed on the basis of changes in inhibitor sensitivity [40]. The M64 residue has been subjected to mutagenesis in *E. coli* previously, and according to capsaicin inhibition data it is not involved in ubiquinone binding [25]. So whereas reports on the effects on the human enzyme and its bacterial counterpart are discrepant, the present results demonstrate a 1.4-fold increase in the K_m for DB in response to the M64V replacement in *E. coli* (Table 3).

It is evident that this domain of NuoJ/ND6 that harbors many disease-associated mutations has some relations to ubiquinone binding site(s). In order to understand this relation better, the mutant with the largest change in ubiquinone affinity, namely NuoJ-M72V, was tested for changes in inhibitor sensitivity with several classes of complex I inhibitors. Unlike the C-type inhibitor VNA, the inhibitory action of piericidin A, which belongs to class I/type-A, and stigmatellin and myxothiazol did not affect the mutants in any different manner from the controls. Since class I/type-A inhibitors, which are quinone-like, and C-type inhibitors do not compete with each other for binding[36], it is

plausible that the C-type inhibitors are bound more distantly in the ubiquinone cavity, at sites leading to the actual active site. Annonin VI is considered a class I/type-A inhibitor [41], but contrary to piericidin A, it was found here to bind to the NuoJ-M72V mutant enzyme with lower affinity than the control (Table 4). The apparent discrepancy in binding between these two inhibitors can be explained by the rather long structure of the annonin VI molecule, with the plausible protein interacting atoms well spaced out. Therefore this inhibitor molecule could interact in both type-A and type-C inhibitor binding domains. This is not in contradiction with the previous work of Okun and co-workers [36], where displacement of the rather short type-A inhibitor 2-decyl-4-quinazolinyl amine was not observed with the type-C inhibitor CC 44. In conclusion, NuoJ-M72V changes the binding affinity of inhibitors that interact with the type-C binding domain. The stable binding of the ubiquinone head group in NuoJ/ND6 is unlikely to be due to the low magnitude of the DB affinity changes and the inhibitor sensitivity pattern observed in the present study. More probably, NuoJ/ND6 might be lining the cavity leading to the actual binding site and providing only transitory interaction with the ubiquinone head group (Figure 4). It was proposed earlier by DeHaan et al. [42] that single amino acid substitutions in ND6 may perturb the secondary structure of the transmembrane helices, thereby causing long-ranging structural derangements. We consider this option unlikely, because none of the mutations introduced should result in steric congestion, due to the smaller size of the amino acid introduced as compared with the wild type, and because the observed changes in inhibitor binding can be assigned to a certain class of inhibitors, whereas larger changes in protein structure would be anticipated to affect the closely-situated type-A inhibitor binding site as well.

(Place Figure 4 here.)

One of the novel findings of the present work is the substrate inhibition by DB in the Y59C mutant. Substrate inhibition by exogenous short-chain ubiquinones (DB, Q_2 and Q_1) has been reported for the LHON-associated ND1-A52T mutation in mitochondrial membrane preparations from lymphoblasts [15], and in the presence of ND6-A72V substitution (see above). Substrate inhibition by ubiquinone could be involved in the pathogenesis of LHON, although Q_{10} did not behave in the same way as its analogues with shorter side-chains that were used in enzyme assays in the presence of the 3460/ND1-A52T mutation [15]. Congruently with this, we found higher enzyme activity for the Y59C mutant when endogenous ubiquinone Q_9 was used by the enzyme than with DB. Filling the binding cavity with the long isoprenoid tail of the $Q_{9\text{-}10}$ molecule could disable additional binding of ubiquinone, while the shorter tail structures of DB, Q_1 or Q_2 might allow the binding of another molecule, and high secondary binding affinity in some mutants could lead to the observed substrate inhibition. Despite the lack of substrate inhibition with endogenous ubiquinone, the phenomenon observed here may provide

crucial information on the defect in these mutant enzymes under normal respiration conditions that ultimately presents itself as LHON in humans. If short-chained ubiquinones present higher secondary binding affinities for the substrate in the long binding cavity, then endogenous ubiquinone will also be subject to stronger intermediate binding interaction within the substrate binding cavity. This could lead to improper channeling of the enzyme for ubiquinone, and, in parallel to the mutants, a lowering of the ubiquinone binding affinity. Both may lead to lower occupancy of the actual ubiquinone reduction site, with potentially disastrous consequences for the retinal ganglion cells, by promoting the production of reactive oxygen species with consequent protein, lipid and DNA modification, impairment of energy production, and as a result, a higher probability of apoptosis. This hypothesis requires further testing, however. It is uncertain whether the altered ubiquinone interaction with complex I alone is sufficient for development of the disease, but the incomplete penetrance of the disease, gender bias, sudden onset of the symptoms and restriction of the affected tissue to a certain cell type are suggestive of other, currently unknown, genetic and/or environmental factors that could also be involved in the presentation of the disease.

(Place Table 5 here.)

In evaluating the effects of a pathogenic mtDNA mutation at the enzymatic level in a bacterial model, one of the main concerns must be the relevance of the results to mitochondrial disease. We compared the effects of NuoJ mutations in *E. coli* with human disease phenotypes caused by equivalent mutations and two LHON mutations in other subunits (Table 5). The clinical phenotype variables evaluated were, first, the presence of other neurological manifestations in addition to LHON, second, disease penetrance and its dependence on gender in the affected families, and, third, the occurrence of visual recovery. This comparison shows that although LHON patients with M64V substitution in the ND6 subunit are less severely affected than patients with the Y59C or A72V mutations, no substantial difference in disease penetrance or its male predominance is detectable. The infrequent visual recovery and the occurrence of additional neurological symptoms in the Y59C and A72V mutations seem, however, to be linked to poorer complex I and/or NDH-1 activity. In addition, the DB-binding properties were more severely hampered in the *E.coli* homologues of the Y59C and A72V mutants than in M64V. The effects on the NDH-1 activity of *E. coli* mutations homologous to the ND6 substitutions M64V and A72V are evidently congruent to those occurring in the mitochondrion, and therefore it is reasonable to expect that this will also hold good for the Y59C mutation, for which no reports on complex I activity in the mitochondria of patients are currently available.

Substitution of phenylalanine for Y109 was initially selected as a neutral control, but the surprising effects of this substitution on the ubiquinone affinity gave us other thoughts. In addition, the close proximity of Y109 to the 14340/ND6-V112M mutation site associated with aminoglycoside-induced or non-aminoglycoside-related sensorineural hearing impairment [43] suggests that this region is of functional significance. A double mutant M64V/M72A was generated to examine whether a methionine in either of these positions is a prerequisite for proper complex I function. The background for this assumption was the observation that whereas human ND6 has a Met residue in position 64 and Ala at 72, the highly homologous NDH-1 from the soil bacterium *Paracoccus denitrificans* has Ala in position 64 and Met at 72 in its equivalent subunit Nqo10 (Figure 1), while in NuoJ of *E. coli*, the model system used here, there are Met residues in both positions, 64 and 72. The respiratory defects caused by the single M64V and M72A mutations in NuoJ were not cumulative as expected, and K_m for DB was in the same range as for M64V and M72A. Contrary to single M64V and M72V mutations, the double mutant did, however, show some tendency for substrate inhibition (Table 3). Co-occurrence of the two mutations in the same protein domain seems to have more drastic effects on the enzyme than the occurrence of either mutant alone, as expected.

This bacterial model for LHON-associated mutations in the mtDNA gene of the ND6 subunit of complex I turned out to be a useful tool for analyzing the effects of these mutations at the enzymatic level. This same approach is applicable to the study of other mtDNA mutations, including the rare ones, and may serve to reveal not only the mechanism underlying the pathogenesis of LHON but also the function of complex I. We hope that this model system will prove useful in the search of suitable therapeutic molecules or remedies for this disease.

ACKNOWLEDGEMENTS

This investigation was supported by grants from the Academy of Finland Council of Health, Sigrid Juselius Foundation (I.H.), the Eye Foundation (Silmäsäätiö) and the Evald and Hilda Nissi Foundation (M.K.). The skilful technical assistance of Aila Holappa and Raija Pietilä is gratefully acknowledged.

References

1 Nikoskelainen, E., Hoyt, W. F., and Nummelin, K. (1983) Ophthalmoscopic findings in Leber's hereditary optic neuropathy. II. The fundus findings in the affected family members. Arch.Ophthalmol. **101**, 1059-1068

2 Johns, D. R., Heher, K. L., Miller, N. R., and Smith, K. H. (1993) Leber's hereditary optic neuropathy. Clinical manifestations of the 14484 mutation. Arch.Ophthalmol. **111**, 495-498

3 Wallace, D. C., Singh, G., Lott, M. T., Hodge, J. A., Schurr, T. G., Lezza, A. M., Elsas, L. J., and Nikoskelainen, E. K. (1988) Mitochondrial DNA mutation associated with Leber's hereditary optic neuropathy. Science. **242**, 1427-1430

4 Man, P. Y., Turnbull, D. M., and Chinnery, P. F. (2002) Leber hereditary optic neuropathy. J.Med.Genet. **39**, 162-169

5 Hinchliffe, P. and Sazanov, L. A. (2005) Organization of iron-sulfur clusters in respiratory complex I. Science. **309**, 771-774

6 Bogachev, A. V., Murtazina, R. A., and Skulachev, V. P. (1996) H^+/e^- stoichiometry for NADH dehydrogenase I and dimethyl sulfoxide reductase in anaerobically grown Escherichia coli cells. J.Bacteriol. **178**, 6233-6237

7 Carroll, J., Fearnley, I. M., Shannon, R. J., Hirst, J., and Walker, J. E. (2003) Analysis of the subunit composition of complex I from bovine heart mitochondria. Mol.Cell Proteomics. **2**, 117-126

8 Friedrich, T., Steinmuller, K., and Weiss, H. (1995) The proton-pumping respiratory complex I of bacteria and mitochondria and its homologue in chloroplasts. FEBS Lett. **367**, 107-111

9 Anderson, S., Bankier, A. T., Barrell, B. G., de Bruijn, M. H., Coulson, A. R., Drouin, J., Eperon, I. C., Nierlich, D. P., Roe, B. A., Sanger, F., Schreier, P. H., Smith, A. J., Staden, R., and Young, I. G. (1981) Sequence and organization of the human mitochondrial genome. Nature. **290**, 457-465

10 DiBernardo, S. D., Yano, T., and Yagi, T. (2000) Exploring the membrane domain of the reduced nicotinamide adenine dinucleotide-quinone oxidoreductase of Paracoccus denitrificans: characterization of the NQO7 subunit. Biochemistry **39**, 9411-9418

11 Carelli, V., Ross-Cisneros, F. N., and Sadun, A. A. (2004) Mitochondrial dysfunction as a cause of optic neuropathies. Prog.Retin.Eye Res. **23**, 53-89

12 Chinnery, P. F., Brown, D. T., Andrews, R. M., Singh-Kler, R., Riordan-Eva, P., Lindley, J., Applegarth, D. A., Turnbull, D. M., and Howell, N. (2001) The mitochondrial ND6 gene is a hot spot for mutations that cause Leber's hereditary optic neuropathy. Brain. **124**, 209-218

13 Valentino, M. L., Barboni, P., Ghelli, A., Bucchi, L., Rengo, C., Achilli, A., Torroni, A., Lugaresi, A. , Lodi, R., Barbiroli, B., Dotti, M., Federico, A., Baruzzi, A., and Carelli, V. (2004) The ND1 gene of complex I is a mutational hot spot for Leber's hereditary optic neuropathy. Ann.Neurol. **56**, 631-641

14 Majander, A., Huoponen, K., Savontaus, M. L., Nikoskelainen, E., and Wikström, M. (1991) Electron transfer properties of NADH:ubiquinone reductase in the ND1/3460 and the ND4/11778 mutations of the Leber hereditary optic neuroretinopathy (LHON). FEBS Lett. **292**, 289-292

15 Majander, A., Finel, M., Savontaus, M. L., Nikoskelainen, E., and Wikström, M. (1996) Catalytic activity of complex I in cell lines that possess replacement mutations in the ND genes in Leber's hereditary optic neuropathy. Eur.J.Biochem. **239**, 201-207

16 Smith, P. R., Cooper, J. M., Govan, G. G., Harding, A. E., and Schapira, A. H. (1994) Platelet mitochondrial function in Leber's hereditary optic neuropathy. J.Neurol.Sci. **122**, 80-83

17 Baracca, A., Solaini, G., Sgarbi, G., Lenaz, G., Baruzzi, A., Schapira, A. H., Martinuzzi, A., and Carelli, V. (2005) Severe impairment of complex I-driven adenosine triphosphate synthesis in leber hereditary optic neuropathy cybrids. Arch.Neurol. **62**, 730-736

18 Komaki, H., Akanuma, J., Iwata, H., Takahashi, T., Mashima, Y., Nonaka, I., and Goto, Y. (2003) A novel mtDNA C11777A mutation in Leigh syndrome. Mitochondrion. **2**, 293-304

19 Wong, A., Cavelier, L., Collins-Schramm, H. E., Seldin, M. F., McGrogan, M., Savontaus, M. L., and Cortopassi, G. A. (2002) Differentiation-specific effects of LHON mutations introduced into neuronal NT2 cells. Hum.Mol.Genet. **11**, 431-438

20 Beretta, S., Mattavelli, L., Sala, G., Tremolizzo, L., Schapira, A. H., Martinuzzi, A., Carelli, V., and Ferrarese, C. (2004) Leber hereditary optic neuropathy mtDNA mutations disrupt glutamate transport in cybrid cell lines. Brain. **127**, 2183-2192

21 Danielson, S. R., Wong, A., Carelli, V., Martinuzzi, A., Schapira, A. H., and Cortopassi, G. A. (2002) Cells bearing mutations causing Leber's hereditary optic neuropathy are sensitized to Fas-Induced apoptosis. J.Biol.Chem. **277**, 5810-5815

22 Ghelli, A., Zanna, C., Porcelli, A. M., Schapira, A. H., Martinuzzi, A., Carelli, V., and Rugolo, M. (2003) Leber's hereditary optic neuropathy (LHON) pathogenic mutations induce mitochondrial-dependent apoptotic death in transmitochondrial cells incubated with galactose medium. J.Biol.Chem. **278**, 4145-4150

23 Bandelt, H. J., Yao, Y. G., Salas, A., Kivisild, T., and Bravi, C. M. (2007) High penetrance of sequencing errors and interpretative shortcomings in mtDNA sequence analysis of LHON patients. Biochem.Biophys.Res.Commun. **352**, 283-291

24 Kervinen, M., Pätsi, J., Finel, M., and Hassinen, I. E. (2004) A pair of membrane-embedded acidic residues in the NuoK subunit of Escherichia coli NDH-1, a counterpart of the ND4L subunit of the mitochondrial complex I, are required for high ubiquinone reductase activity. Biochemistry. **43**, 773-781

25 Kao, M. C., Di Bernardo, S., Nakamaru-Ogiso, E., Miyoshi, H., Matsuno-Yagi, A., and Yagi, T. (2005) Characterization of the membrane domain subunit NuoJ (ND6) of the NADH-quinone oxidoreductase from Escherichia coli by chromosomal DNA manipulation. Biochemistry. **44**, 3562-3571

26 Mitchell, A. L., Elson, J. L., Howell, N., Taylor, R. W., and Turnbull, D. M. (2006) Sequence variation in mitochondrial complex I genes: mutation or polymorphism? J.Med.Genet. **43**, 175-179

27 Oden, K. L., DeVeaux, L. C., Vibat, C. R., Cronan, J. E., Jr., and Gennis, R. B. (1990) Genomic replacement in Escherichia coli K-12 using covalently closed circular plasmid DNA. Gene **96**, 29-36

28 Leif, H., Sled, V. D., Ohnishi, T., Weiss, H., and Friedrich, T. (1995) Isolation and characterization of the proton-translocating NADH: ubiquinone oxidoreductase from Escherichia coli. Eur.J Biochem. **230**, 538-548

29 Kervinen, M., Hinttala, R., Helander, H. M., Kurki, S., Uusimaa, J., Finel, M., Majamaa, K., and Hassinen, I. E. (2006) The MELAS mutations 3946 and 3949 perturb the critical structure in a conserved loop of the ND1 subunit of mitochondrial complex I. Hum.Mol.Genet. **15** , 2543-2552

30 Lowry, O. H., Rosebrough, N. J., Farr, A. L., and Randall, R. J. (1951) Protein measurement with the Folin phenol reagent. J.Biol.Chem. **193**, 265-275

31 Matsushita, K., Ohnishi, T., and Kaback, H. R. (1987) NADH-ubiquinone oxidoreductases of the Escherichia coli aerobic respiratory chain. Biochemistry. **26**, 7732-7737

32 Dixon, M. and Webb, E. C. (1971) Enzymes, Longman, London

33 Bai, Y. and Attardi, G. (1998) The mtDNA-encoded ND6 subunit of mitochondrial NADH dehydrogenase is essential for the assembly of the membrane arm and the respiratory function of the enzyme. EMBO J. **17**, 4848-4858

34 Moreno-Loshuertos, R., Acin-Perez, R., Fernandez-Silva, P., Movilla, N., Perez-Martos, A., Rodriguez, d. C., Gallardo, M. E., and Enriquez, J. A. (2006) Differences in reactive oxygen species production explain the phenotypes associated with common mouse mitochondrial DNA variants. Nat.Genet. **38**, 1261-1268

35 Pye, D., Kyriakouli, D. S., Taylor, G. A., Johnson, R., Elstner, M., Meunier, B., Chrzanowska-Lightowlers, Z. M., Taylor, R. W., Turnbull, D. M., and Lightowlers, R. N. (2006) Production of transmitochondrial cybrids containing naturally occurring pathogenic mtDNA variants. Nucleic Acids Res. **34**, e95

36 Okun, J. G., Lummen, P., and Brandt, U. (1999) Three classes of inhibitors share a common binding domain in mitochondrial complex I (NADH:ubiquinone oxidoreductase). J.Biol.Chem. **274**, 2625-2630

37 Zickermann, V., Bostina, M., Hunte, C., Ruiz, T., Radermacher, M., and Brandt, U. (2003) Functional implications from an unexpected position of the 49-kDa subunit of NADH:ubiquinone oxidoreductase. J.Biol.Chem. **278**, 29072-29078

38 Brandt, U. (2006) Energy Converting NADH:Quinone Oxidoreductase (Complex I). Annu.Rev.Biochem. **75**, 69-92

39 Jun, A. S., Trounce, I. A., Brown, M. D., Shoffner, J. M., and Wallace, D. C. (1996) Use of transmitochondrial cybrids to assign a complex I defect to the mitochondrial DNA-encoded NADH dehydrogenase subunit 6 gene mutation at nucleotide pair 14459 that causes Leber hereditary optic neuropathy and dystonia. Mol.Cell Biol. **16**, 771-777

40 Carelli, V., Ghelli, A., Bucchi, L., Montagna, P., De Negri, A., Leuzzi, V., Carducci, C., Lenaz, G., Lugaresi, E., and Degli, E. M. (1999) Biochemical features of mtDNA 14484 (ND6/M64V) point mutation associated with Leber's hereditary optic neuropathy. Ann.Neurol. **45**, 320-328

41 Friedrich, T., van Heek, P., Leif, H., Ohnishi, T., Forche, E., Kunze, B. , Jansen, R., Trowitzsch-Kienast, W., Hofle, G., Reichenbach, H., and Weiss, H. (1994) Two binding sites of inhibitors in NADH: ubiquinone oxidoreductase (complex I). Relationship of one site with the ubiquinone-binding site of bacterial glucose:ubiquinone oxidoreductase. Eur.J.Biochem. **219**, 691-698

42 DeHaan, C., Habibi-Nazhad, B., Yan, E., Salloum, N., Parliament, M., and Allalunis-Turner, J. (2004) Mutation in mitochondrial complex I ND6 subunit is associated with defective response to hypoxia in human glioma cells. Mol.Cancer. **3**, 19

43 Zhao, L., Wang, Q., Qian, Y., Li, R., Cao, J., Hart, L. C., Zhai, S., Han, D., Young, W. Y., and Guan, M. X. (2005) Clinical evaluation and mitochondrial DNA sequence analysis in two Chinese families with aminoglycoside-induced and non-syndromic hearing loss. Biochem.Biophys.Res.Commun. **336**, 967-973

44 Wissinger, B., Besch, D., Baumann, B., Fauser, S., Christ-Adler, M., Jurklies, B., Zrenner, E., and Leo-Kottler, B. (1997) Mutation analysis of the ND6 gene in patients with Lebers hereditary optic neuropathy. Biochem.Biophys.Res.Commun. **234**, 511-515

45 Leo-Kottler, B., Christ-Adler, M., Baumann, B., Zrenner, E., and Wissinger, B. (1996) Leber's hereditary optic neuropathy: clinical and molecular genetic results obtained in a family with a new point mutation at nucleotide position 14498 in the ND 6 gene. Ger J.Ophthalmol. **5**, 233-240

46 Mackey, D. and Howell, N. (1992) A variant of Leber hereditary optic neuropathy characterized by recovery of vision and by an unusual mitochondrial genetic etiology. Am.J.Hum.Genet. **51**, 1218-1228

47 Brown, M. D., Trounce, I. A., Jun, A. S., Allen, J. C., and Wallace, D. C. (2000) Functional analysis of lymphoblast and cybrid mitochondria containing the 3460, 11778, or 14484 Leber's hereditary optic neuropathy mitochondrial DNA mutation. J.Biol.Chem. **275**, 39831-39836

48 Spruijt, L., Kolbach, D. N., de Coo, R. F., Plomp, A. S., Bauer, N. J., Smeets, H. J., and Die-Smulders, C. E. (2006) Influence of mutation type on clinical expression of Leber hereditary optic neuropathy. Am.J.Ophthalmol. **141**, 676-682

49 Novotny, E. J., Jr., Singh, G., Wallace, D. C., Dorfman, L. J., Louis, A., Sogg, R. L., and Steinman, L. (1986) Leber's disease and dystonia: a mitochondrial disease. Neurology. **36**, 1053-1060

50 Johns, D. R., Smith, K. H., and Miller, N. R. (1992) Leber's hereditary optic neuropathy. Clinical manifestations of the 3460 mutation. Arch.Ophthalmol. **110**, 1577-1581

51 Newman, N. J., Lott, M. T., and Wallace, D. C. (1991) The clinical characteristics of pedigrees of Leber's hereditary optic neuropathy with the 11778 mutation. Am.J.Ophthalmol. **111**, 750-762

52 Kao, M. C., Di Bernardo, S., Matsuno-Yagi, A., and Yagi, T. (2003) Characterization and topology of the membrane domain Nqo10 subunit of the proton-translocating NADH-quinone oxidoreductase of Paracoccus denitrificans. Biochemistry. **42**, 4534-4543

53 Ugalde, C., Triepels, R. H., Coenen, M. J., van den Heuvel, L. P., Smeets, R., Uusimaa, J., Briones, P., Campistol, J., Majamaa, K., Smeitink, J. A., and Nijtmans, L. G. (2003) Impaired complex I assembly in a Leigh syndrome patient with a novel missense mutation in the ND6 gene. Ann.Neurol. **54**, 665-669

54 Ravn, K., Wibrand, F., Hansen, F. J., Horn, N., Rosenberg, T., and Schwartz, M. (2001) An mtDNA mutation, 14453G→A, in the NADH dehydrogenase subunit 6 associated with severe MELAS syndrome. Eur.J.Hum.Genet. **9**, 805-809

55 Baranova, E. A., Holt, P. J., and Sazanov, L. A. (2007) Projection structure of the membrane domain of Escherichia coli respiratory complex I at 8 Å resolution. J.Mol.Biol. **366**, 140-154

Table 1. LHON mutations in the third transmembrane helix of the human ND6 subunit of complex I and mutations introduced into the NuoJ subunit of *E. coli* NDH-1.

T14484C mutation is one of the three common primary LHON-mutations.

Mitochondrial mutations in ND6 and resulting disease			Mutations introduced into *Escherichia coli* NuoJ
Nucleotide change	Residue change	Disease*	
T14498C	Y59C	LHON	Y59C, Y59F
T14484C	M64V	LHON	
C14482G	M64I	LHON	M64V, M64C
C14482A	M64I	LHON	
G14459A	A72V	LDYT	V65G †M72V, M72C, M72A Y109F

*LHON, Leber hereditary optic neuropathy; LDYT, LHON and dystonia.

†There is a Met residue at position 72 in NuoJ of *E. coli,* whereas there is Ala in this position in the human ND6 (Figure 1).

Table 2. Respiratory activities in NuoJ mutants and the control, and their growth capability on malate.

Five colonies for the control and three for each mutant were subjected to membrane isolation and activity analyses (run in triplicate). Units for NADH:O_2, d-NADH:O_2 and d-NADH:HAR activity are nmol min^{-1} mg^{-1}. For growth on malate, which was determined as final attenuance of cultures at 600 nm after 1 day of growth in malate-YE medium, eleven cultures were analyzed for the control, nine for Y59F, eight for M64C, seven for M72V and six for the rest of the mutants. The values are means ± S.E.M.

Mutant	Growth on malate	NADH:O_2	d-NADH:O_2	d-NADH:HAR
Control	0.86 ± 0.05	309 ± 53	184 ± 56	1140 ± 304
Y59C	0.69 ± 0.01	261 ± 39	156 ± 22	1038 ± 93
Y59F	0.16 ± 0.01	242 ± 12	76 ± 6	1056 ± 40
M64V	0.68 ± 0.03	467 ± 72	313 ± 52	2498 ± 278
M64C	0.35 ± 0.08	230 ± 57	90 ± 34	1198 ± 482
M72V	0.22 ± 0.01	228 ± 35	70 ± 8	1141 ± 56
M72A	0.68 ± 0.03	338 ± 78	233 ± 79	1945 ± 517
M72C	0.34 ± 0.01	176 ± 15	86 ± 9	1052 ± 47
M64V/M72A	0.41 ± 0.03	198 ± 19	97 ± 7	645 ± 53
V65G	0.06 ± 0.05	180 ± 17	4 ± 1	939 ± 390
Y109F	0.75 ± 0.01	308 ± 26	207 ± 13	1338 ± 50

Table 3. Kinetic properties of control and NuoJ mutants.

K_m and K_s' values for decylubiquinone and the V_{max} of d-NADH:decylubiquinone oxidoreductase activity were calculated by fitting the data to the equation $v=V_{max}\cdot[S]/(K_m+[S]+([S]^2/K_s'))$, as described under Results. V_{max} of d-NADH:DB activity was normalized to d-NADH:HAR activity to account for variations in expression levels between different membrane batches of individual mutants. Only the mean is shown for K_s', the other values are means ± S.E.M. measured from the same samples as described in Table 2.

Mutant	V_{max}/HAR		K_m (μM)	K_s' (μM)
control	0.216 ± 0.018	(100%)	23 ± 2	4227
Y59C	0.158 ± 0.008	(73%)	22 ± 2	594*
Y59F	0.083 ± 0.003†	(38%)	29 ± 3	1285
M64V	0.180 ± 0.016	(83%)	33 ± 4*	3409
M64C	0.120 ± 0.011†	(56%)	38 ± 2†	4615
M72V	0.114 ± 0.003†	(53%)	39 ± 4†	∞‡
M72A	0.170 ± 0.020	(79%)	46 ± 2†	12430
M72C	0.147 ± 0.008*	(68%)	42 ± 1†	16939
M64V/ M72A	0.264 ± 0.034	(122%)	38 ± 2†	1792
Y109F	0.241 ± 0.016	(112%)	42 ± 4†	5273

*p<0.05, †p<0.01 when compared to control.

‡ No exact value could be calculated because of low affinity.

Table 4. Inhibitor sensitivity in the NuoJ-M72V mutant and wild-type control.

I_{50}, the inhibitor concentration that produces 50% inhibition of the d-NADH:DB activity, was measured at 100 µM DB. Myxothiazol at the concentrations used (5-100 µM) showed a maximal inhibition of d-NADH:DB activity of only 37%, and no difference was observed between the control and the NuoJ-M72V mutant (results not shown). Values are means ± S.D., numbers in parentheses indicate the number of independent experiments.

Inhibitor	I_{50}	
	Control	NuoJ-M72V
Annonin (µg/ml)	0.50 ± 0.06 (n = 2)	0.96 ± 0.20* (n = 4)
VNA (µM)	62 ± 13 (n = 5)	133 ± 24* (n = 2)
Piericidin A (µM)	12	10
Stigmatellin (µM)	22	29
Myxothiazol (µM)	>100	>100

* $p<0.05$

Table 5. Clinical characteristics and complex I/NDH-1 activity of the ND6 subunit-associated LHON mutations generated in this work and common LHON mutations in the ND1 and ND4 subunits.

Number in parenthesis for visual recovery indicates percentage of patients experiencing visual recovery. Complex I (CI) activities are from cybrid cells, no data on complex I activity in patients with C14498T mutation are available. n.a., not applicable.

Subunit	Mutation	Amino acid change	Phenotype	Penetrance (%)		Visual recovery	CI activity (% of control)	References	Present work NDH-1	
				Male	Female				Activity ‡ (% of control)	DB binding
ND6	C14498T	Y59C	LHON	40	25	poor	no data	[44,45]	66	Substrate inhibition
ND6	T14484C	M64V	LHON	50	12	good (37-64%)	90	[2,46-48]	73	K_m 1.4-fold
ND6	G14459A	A72V	LDYT*	52	52	no/poor	70	[39,49]	56 §	K_m 1.7-fold §
			LHON only	29	10					
			Dystonia only	24	38					
			L+D †	n.a.	5					
ND1	G3460A	A52T	LHON	46	19	intermediate (15-20%)	30	[47,48,50]		
ND4	G11778A	R340H	LHON	52	10	intermediate (4-22%)	90-100	[48,51]		

*Leber hereditary optic neuropathy and/or dystonia.

† Leber hereditary optic neuropathy and dystonia.

‡ Ratio of d-NADH:DB to d-NADH:HAR activity at 100 μM DB concentration.

§ Results of NuoJ-M72V mutant.

Legends to figures

Figure 1. Alignment of the region around the third putative transmembrane helix of the human ND6 with selected homologues.

The predicted transmembrane helix in the *E. coli* sequence is underlined[52]. Highly conserved amino acids are highlighted in grey. (▲) denotes residues for which site-directed mutants were constructed in this work. The uppermost line shows substitutions associated with diseases[12,53,54]. The GenBank accession numbers for the sequences are (from top to bottom) ABA08023 (Human), AAV88355 (Bovine), NP_007573 (*Alligator mississippiensis*), NP_059342 (Zebrafish), CAC28088 (*Yarrowia lipolytica*), YP_271941 (*Montastraea franksi*), CAA60351 (Maize chloroplast), P29922 (*Paracoccus denitrificans*), AAA97947 (*Thermus thermophilus*) and NP_416783 (*E. coli*). The alignment was performed with the ClustalW program.

Figure 2. Correlation between growth in a malate-YE medium and d-NADH oxidation activity in *E. coli* mutants.

Cell density was measured as the attenuance of the culture at 600 nm. The curve represents a least-squares fit of the logistic dose response curve $y = (a-d)/[1 + (x/c)^b] + d$. R = 0.796, P<0.001, and the values are means ± S.E.M.

Figure 3. Substrate inhibition in NuoJ-Y59-position mutants.

Representative DB titrations of d-NADH:DB reductase activity in cytoplasmic membranes from the control or mutants at a fixed d-NADH concentration. Activities are given as ratios of d-NADH:HAR reductase activity to eliminate the effect of variations in expression level. The solid curves represent a fit to the equation $v=V_{max}\cdot[S]/(K_m+[S]+([S]^2/K_s'))$, as described under Results. (○) Control; (◇) Y59C; (▽) Y59F.

Figure 4. Proximity relations between the ND6/NuoJ, ND1/NuoH, PSST/NuoB and 49 kDa/NuoD subunits in complex I and tentative location of the inhibitor-sensitive ubiquinone binding site.

ND6 may not participate in ubiquinone binding but it does contribute to a channel through which the binding site becomes accessible. The binding sites for class A/I, B/II and C inhibitors are marked with "a", "b" and "c", respectively. The general shape of the *E. coli* enzyme and the arrangement of the membrane-embedded subunits are from single particle analysis and fragmentation studies performed by Sazanov and coworkers[55].

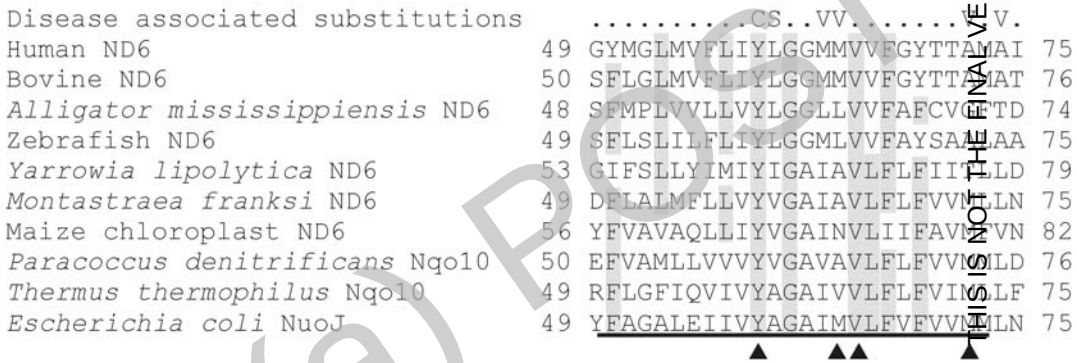

Figure 1. Pätsi et al.

Biochemical Journal Immediate Publication. Published on 26 Sep 2007 as manuscript BJ20070866

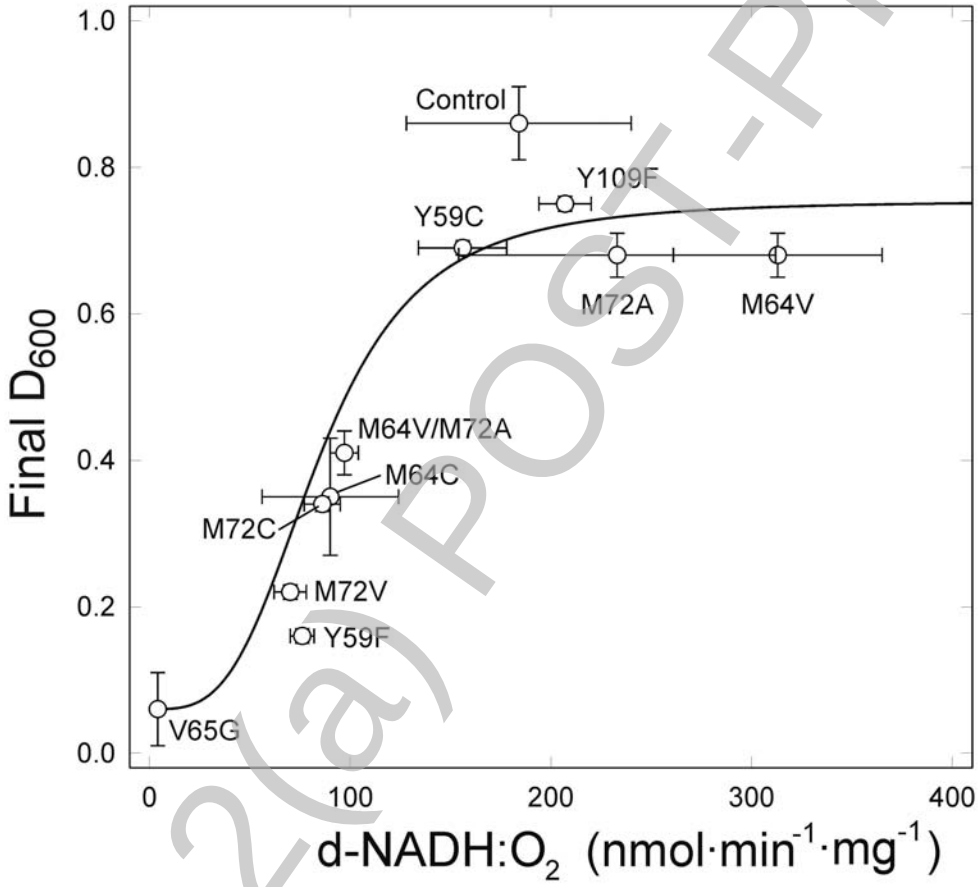

Figure 2. Pätsi et al.

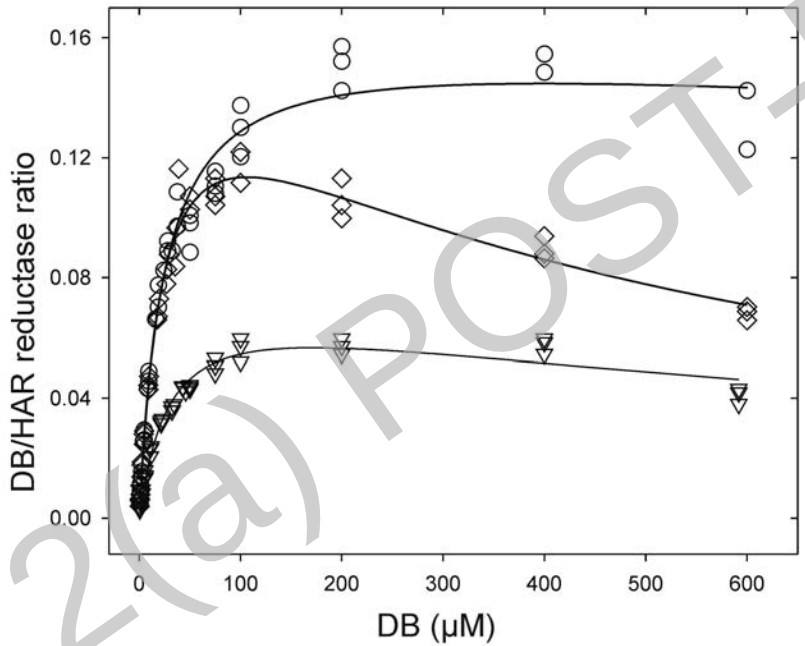

Figure 3. Pätsi et al.

Biochemical Journal Immediate Publication. Published on 26 Sep 2007 as manuscript BJ20070866

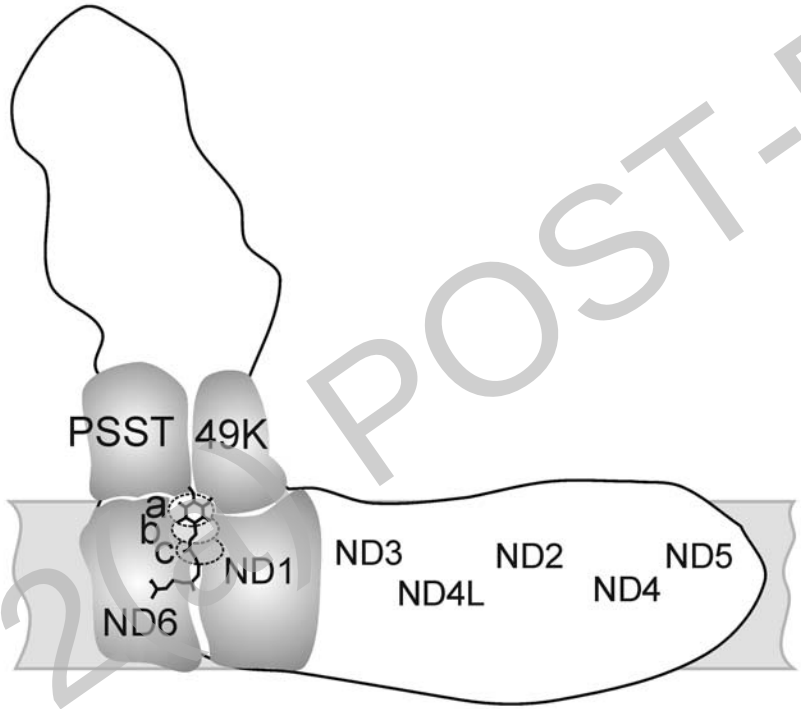

Figure. 4. Pätsi et al.